Improved bathymetric datasets for the shallow water regions in the Indian Ocean

B Sindhu*, I Suresh, A S Unnikrishnan, N V Bhatkar, S Neetu and G S Michael

National Institute of Oceanography, Dona Paula, Goa 403 004, India.
**e-mail: smole@nio.org*

Ocean modellers use bathymetric datasets like ETOPO5 and ETOPO2 to represent the ocean bottom topography. The former dataset is based on digitization of depth contours greater than 200 m, and the latter is based on satellite altimetry. Hence, they are not always reliable in shallow regions. An improved shelf bathymetry for the Indian Ocean region (20°E to 112°E and 38°S to 32°N) is derived by digitizing the depth contours and sounding depths less than 200 m from the hydrographic charts published by the National Hydrographic Office, India. The digitized data are then gridded and used to modify the existing ETOPO5 and ETOPO2 datasets for depths less than 200 m. In combining the digitized data with the original ETOPO dataset, we apply an appropriate blending technique near the 200 m contour to ensure smooth merging of the datasets. Using the modified ETOPO5, we demonstrate that the original ETOPO5 is indeed inaccurate in depths of less than 200 m and has features that are not actually present on the ocean bottom. Though the present version of ETOPO2 (ETOPO2v2) is a better bathymetry compared to its earlier versions, there are still differences between the ETOPO2v2 and the modified ETOPO2. We assess the improvements of these bathymetric grids with the performance of existing models of tidal circulation and tsunami propagation.

1. Introduction

Bathymetric datasets form a major input for ocean models. A variety of bathymetric datasets with different coverages, resolutions, and accuracies are now available. Among these are the ETOPO5 (National Geophysical Data Centre (NGDC) 1988) and the ETOPO2v2 (NGDC 2006) bathymetric grids, both of which are now in wide use.

ETOPO5 is a 5 arc minute bathymetry grid produced by combining the ocean depth values obtained from DBDB-5 (US National Geospatial-Intelligence Agency 1994) with the land elevation data obtained from different sources. The DBDB-5 (Digital Bathymetric Data Base 5) dataset was generated by digitizing the depth contours above 200 m from hydrographic charts of nominally 1:4,000,000 scale. The digitized values were gridded to a 5 arc minute grid using a multi-stage, minimum-curvature, spline interpolation algorithm. Digitization was carried out only for depths greater than 200 m as DBDB-5 was designed to be used only as a deep-water data base (Goodwillie 2003). Hence, the ETOPO5 dataset is not reliable in regions where the depth is less than 200 m.

ETOPO2v2 dataset is a newly constructed global elevation database gridded at 2 arc minute resolution. The updated version, released in 2006, has many improvements over the earlier version released in 2001 (http://www.ngdc.noaa.gov/mgg/fliers/06mgg01.html). The different data sources used to derive the updated ETOPO2v2 are Smith/Sandwell database (Smith and Sandwell 1997), the "Global Land One-kilometer Base Elevation" database (GLOBE) (Hastings *et al* 1998), the International Bathymetric Chart of the Arctic Ocean (IBCAO; Jakobsson *et al* 2000),

Keywords. Shelf bathymetry; Indian Ocean; ETOPO; Red Sea; Persian Gulf; Arabian Sea; Bay of Bengal; Andaman Islands.

J. Earth Syst. Sci. **116**, No. 3, June 2007, pp. 261–274

Table 1. *List of hydrographic charts used for digitization, their natural scale, and year of publication for different regions in the Indian Ocean.*

	Charts	Scale	Year
1	Walvis Bay to Lorenco Marques	1:35,00,000	1975
2	Lorenco Marques to Mogadiscio	1:35,00,000	1971
3	Indian Ocean: Western portion	1:100,00,000	1979
4	Gulf of Aden: Eastern portion including Socatra Island	1:750,000	1982
5	Gulf of Aden and southern part of Red Sea	1:750,000	1978
6	Red Sea	1:22,50,000	1973
7	Arabian Sea	1:35,00,000	1974
8	Strait of Hormuz to Qatar	1:750,000	1982
9	Qatar to Shatt Al Arab	1:750,000	1982
10	Muscat to Mumbai (Bombay)	1:15,00,000	1980
11	Gwadar to Dwarka	1:750,000	1979
12	Mumbai (Bombay) to Cape Comorin	1:15,00,000	1980
13	Cochin to Vishakhapatnam	1:15,00,000	1974
14	Bay of Bengal: Northern side (Krishnapatnam to Bassein river)	1:15,00,000	1976
15	Andaman Sea	1:15,00,000	1979
16	Maldive Islands to Sumatra	1:35,00,000	1973
17	South China Sea	1:35,00,000	1976
18	Cora Divh to Elikalpeni bank	1:500,000	1983
19	Central Lakshwadeep	1:300,000	1983
20	Ihavandiffulu atoll to Horsburgh atoll	1:300,000	1981
21	Horsburgh atoll to Haddummati atoll	1:300,000	1982
22	Haddummati atoll to Addu atoll	1:300,000	1981
23	Chagos Archipelago	1:375,000	1984
24	Chagos Archipelago to Malagasy	1:35,00,000	1974

NGDC Coastal Relief Model (Divins and Metzger 2003), NGDC Great Lakes Bathymetric Data (NOAA 2001), and Caspian Sea bathymetry. ETOPO2 is based on satellite altimetry and works best in deep-water regions. In shallow waters, the gravitational effects are too small for the satellite measurements to be reliable. Hence, ETOPO2 is not always reliable in shallow-water regions (http://www.ngdc.noaa.gov/mgg/global/relief/ETOPO2/ETOPO2-2001).

The shallow-water bathymetric data are usually collected and managed by regional organizations for regional interests. Hence, the shallow-water bathymetric datasets are often not as co-ordinated internationally and not as standardized as deep-water datasets. This leads to the use of different sources of bathymetry data by ocean modellers. For example, Unnikrishnan *et al* (1999) used a non-linear 2-D tidal model to simulate tides and tidal circulation in the Gulf of Khambhat, Bombay High, and surrounding areas. They digitized the hydrographic charts of the region to get a more accurate bathymetry to improve model results. Fujii and Satake (2007) noticed high depth values in the ETOPO2 (2001 version) dataset near the Myanmar coast of Andaman Islands. They hence digitized depth points from nautical charts and combined with the ETOPO2 dataset for their tsunami propagation model. The absence of a common dataset for shallow regions leads to bathymetry becoming a 'variable' in model simulations. Hence, there is a need for a common dataset for shallow waters in the Indian Ocean. This need has become urgent after the disastrous tsunami of 26 December 2004 that occurred in the Indian Ocean. Tsunami simulations are critically dependent on the bathymetry used, as are the source-region estimates based on backward ray tracing (Lay *et al* 2005a, b; Neetu *et al* 2005). Therefore, there is a need to generate reliable bathymetry on the continental shelf of the Indian Ocean to eliminate a potential source of differences among various model studies.

In this work, we digitize the depth contours less than 200 m from hydrographic charts for the Indian Ocean region (20°E to 112°E and 38°S to 32°N). We modify the original ETOPO5 and the ETOPO2v2 bathymetric grids in shallow-water regions using the digitized data and demonstrate the improvements of the modified datasets over the original ETOPO datasets. The modified ETOPO5 and the modified ETOPO2 datasets provide ocean

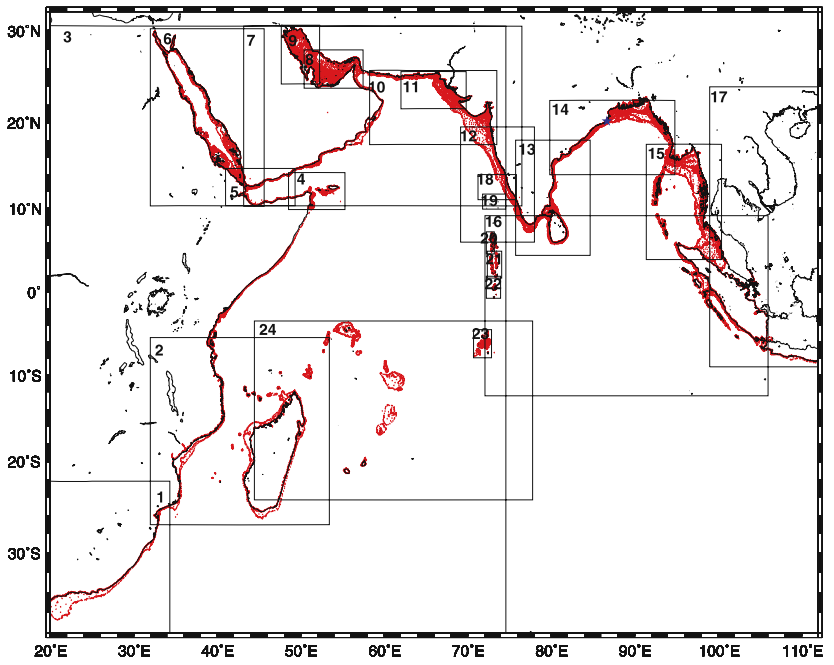

Figure 1. The boxes in the map show the regions from which the hydrographic charts were digitized. The number in each box corresponds to the number given in table 1. The digitized values are also plotted. The asterisk (blue) shows the location of Paradip (20°16′ N, 86°42′ E) (see figure 2).

modellers with a common dataset for the shallow regions in the Indian Ocean.

2. Data and methodology

2.1 *Generation of improved bathymetric grids*

Hydrographic charts (published by the National Hydrographic Office (NHO), Dehradun, India; NHO was known as the Naval Hydrographic Office till 1998) used in the present work for digitization are listed in table 1 and shown in figure 1. The nautical charts and the allied nautical publications produced by NHO have raised the reputation of the organisation all over the world for their accurateness (Ahuja 2000). The databases used in the preparation of these charts are obtained from different sources of information like hydrographic survey, local survey, ocean soundings, earlier editions of nautical charts, coastal survey, and tidal data (Vatsa *et al* 2002). Thus, the accuracy and the adequacy of the hydrographic charts depend on the quality of data collected during the survey (Vatsa *et al* 2002). The International Hydrographic Organization (IHO) has defined minimum standards for hydrographic surveys (such as positional accuracy, sounding accuracy, and sounding density) in its special publication 44 (S-44). These standards are to be applied to the hydrographic charts all over the world (Van der Wal and Pye 2003). The first edition of S-44 was published in 1968 with subsequent editions in 1982 and 1987. These three editions were similar as they were meant for the surveys carried out for the preparation of nautical charts, which were generally used for marine navigation (Mills 1998). These standards require that at least 95% of the positions for the soundings in shallow water should lie within 1.5 mm of the true positions at the scale of the survey (Van der Wal and Pye 2003). Thus, for a 1:10,000 scale of survey, soundings are to be located within 15 m of their true position with a confidence level of 95%. According to the third edition of S-44 (IHO 1987), at least 90% of the total errors in measuring depths should not exceed 30 cm for depths less than 30 m and 1% of depths for depths greater than 30 m (Mills 1998). Also, the distance between each sounding line should not be more than 1 cm at the scale of survey and the sounding interval should not exceed 4 to 6 mm at the survey scale. NHO follows these standards and publishes the charts and other publications in total compliance with the specifications of IHO. NHO also maintains constant interaction with other NHO and the IHO in order to ensure strict standards in products and services (http://indiannavy.nic.in/methodology.htm). The hydrographic charts used in the present work for digitization were published during 1971–1982. Prior to installation of the automated cartographic system in NHO during 1981 (Vatsa and Rajesh Kumar 2002), the conventional hand-drawn method was used to draw contours from

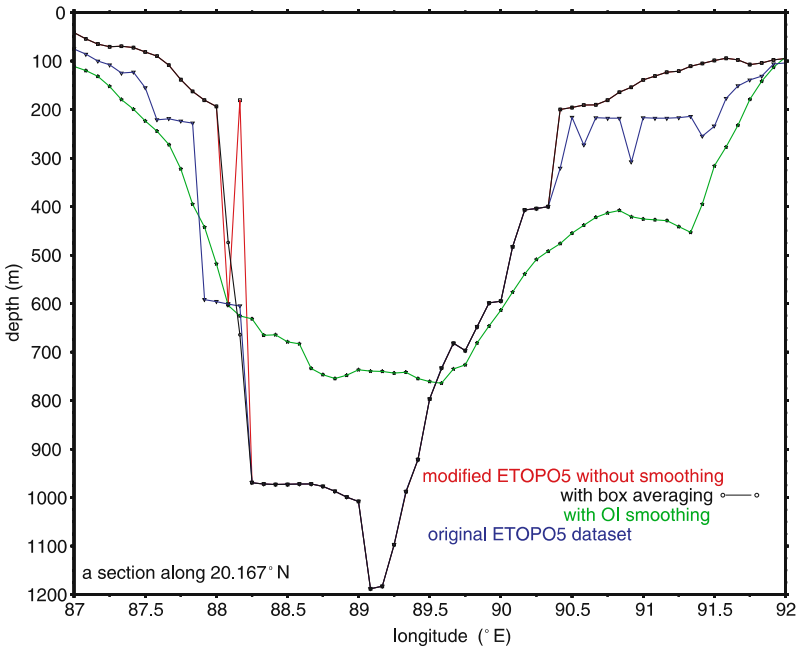

Figure 2. A section of the ocean bottom topography off Paradip (see figure 1), showing the comparison between different blending techniques used: simple averaging (○—○) and optimal interpolation (green line). Also plotted is the original ETOPO5 (blue line) and modified dataset before applying smoothing (red line).

the lines of soundings obtained using the echo sounder trace, the soundings log, and the track chart.

2.1.1 *Digitization of the charts*

Digitization of the maps was carried out using the GRASS (Geographic Resources Analysis Support System) GIS (Geographic Information System) (GRASS Development Team 2005) software. It is an open-source, free software that is readily available on the web at http://grass.itc.it. While importing the non-georeferenced scanned maps into GRASS, they were assigned X–Y projection and the grid resolution was defined to be one pixel. The unreferenced map was then geo-coded by defining nine ground control points (GCPs). After setting at least three reference points, the accuracy of the GCPs was checked using the software's in-built function to calculate the root mean square (RMS) error. The RMS error is acceptable if it is less than half of the grid resolution (Neteler and Mitasova 2002) (i.e., RMS should be less than 0.5). There was also an option to deactivate a control point if it deviated considerably from the other points. The software also allowed quality control in which the geo-coded points could be checked against the actual points in the scanned maps. Thus, the geo-coding was done with care and the RMS error obtained was less than 0.2. The results so obtained would be highly accurate.

The contours digitized from the small scale charts (1:2,250,000–10,000,000) were 30 m and 200 m and those from the large scale charts (1:300,000–1,500,000) were 5, 10, 20, 30, 50, 100, and 200 m. To ensure accurate interpolation, the digitization was carried out at very close intervals to capture the trends in the contours and to obtain sufficiently dense data. All the sounding depths less than 200 m were also digitized.

2.1.2 *Gridding the digitized data*

The digitized data thus obtained were averaged using a simple box-averaging process called *blockmean* that is available in the GMT (Generic Mapping Tools) (Wessel and Smith 1998) package. The box size defined for averaging was equal to target grid size. The averaged data were then gridded on a 5 arc minute latitude–longitude grid using the *surface* program (Wessel and Smith 1995) in the GMT package. The *surface* program is a generalization of the minimum curvature algorithm. As mentioned earlier, DBDB5 (the major source of data for ETOPO5 data set) was gridded using the minimum curvature spline algorithm, which is of the high-order class and can cause undesired oscillations and false local maxima or minima (Smith and Wessel 1990). The *surface* program, used in the present work, not only suppresses these effects, but also prevents extrapolation by allowing the addition of a tension factor and bound constraints. The tension factor, fixed at 0.8, was chosen in such a

way that the difference between the gridded data and the nearest digitized values was minimum in the least squares sense. In the present work, the closed polygons with 200 m contour form the bound constraints; the values outside the polygons were masked, so that the *surface* program did not produce any extrapolation. The values extrapolated on land were also masked using the options available in the GMT package.

2.1.3 *Blending the original and the gridded datasets*

The gridded data derived with the same resolution as that of ETOPO5 was combined with the original ETOPO5 dataset (masked for the land elevations and depths shallower than 200 m) to produce a better quality bathymetric dataset. The dataset obtained by simply merging the original ETOPO5 with the digitized dataset showed some unrealistic features near the 200 m contour (figure 2), implying the need to ensure a smooth transition between the two datasets. We tried out various techniques to blend these two datasets, but none of them performed well, including the optimal interpolation method (figure 2). The optimal interpolation method works best for a smoothly varying field and is dependent on the first-guess field. Since the bathymetric data shows sharp gradients, especially near the continental rise and shelf break where the 200 m contour generally falls, optimal interpolation was found to be inappropriate in this case. Hence, we blended these datasets using a simple box-averaging process. In this method, we first picked up those grid points which showed spurious spikes (due to the merging of datasets) in the dataset and then replaced the depth value at each of these points by the average of the depth values over a box of size 10 minutes (4 minutes for ETOPO2 dataset) around it. The average was computed only over the ocean points and did not include the land points in the box. This method chopped off the unrealistic spikes in the dataset and kept the depths at other grid points unchanged (figure 2). Thus, we obtained a 'modified ETOPO5' bathymetry which was identical to the original ETOPO5 in the deep ocean (depth greater than 200 m), but contained more accurate depths derived from hydrographic charts for shallow waters (less than 200 m).

The digitized data were also gridded to 2 arc minutes and combined with the ETOPO2v2 dataset (masked for the land elevations and depths shallower than 200 m) to obtain a 'modified ETOPO2' dataset by following the same procedures as those used for deriving the modified ETOPO5 dataset.

Though the region covered by the modified ETOPO5 and ETOPO2 datasets extend up to 112°E, we were concerned with the improvements only in the Indian Ocean region and therefore, masked the China Sea region in the modified datasets. The modified datasets are valid only for the Indian Ocean region.

2.2 *Models used*

In order to assess the improvement of the two modified bathymetric datasets over the original ETOPO5 and the ETOPO2v2 datasets, we ran the existing two-dimensional tidal model (Unnikrishnan *et al* 1999) and a tsunami model using these bathymetric datasets.

The tidal model developed by Unnikrishnan *et al* (1999) is used to simulate the tides and the tidal circulation in the Gulf of Khambhat, Bombay High, and the surrounding areas. This model was run on 5 arc minute resolution for the same domain using the original ETOPO5 and the modified ETOPO5 bathymetric grids separately without changing any other model parameters. Similar runs were carried out on 2 arc minute spatial resolution with the ETOPO2v2 and the modified ETOPO2 datasets separately. We evaluated the accuracy of these bathymetric grids by comparing the model results (sea surface elevation and vertically averaged current) with the observations. Tide-gauge sea-surface elevation at Veraval and Mumbai (Apollo Bandar) and current-meter measurements in the Bombay High (19°24.5′N and 71°2.5′E) region during 24 December 1981 to 03 January 1982, which were used by Unnikrishnan *et al* (1999), were also used here for the comparison. We computed the vertically averaged cross-shore (u) and alongshore (v) components of the currents from the current-meter measurements available at four depths (30, 45, 60, and 75 m). These vertically averaged components include the currents generated by other processes such as winds, etc., in addition to tide-driven currents, whereas the currents simulated using the tidal model are driven only by tides. In order to compare the observed currents with the simulated currents, the tidal currents had to be extracted from the measured currents, for which we applied a high-pass filter with cut off at $0.75\,\mathrm{day}^{-1}$ to the vertically averaged current in order to remove the low-frequency component.

Tsunami wave propagation depends mainly on ocean bathymetry. In order to accurately evaluate the tsunami propagation velocity and hence the tsunami arrival times at different locations, precise bathymetry is required (Satake 1988). Using the new bathymetric dataset, we carried out numerical simulation of the 26 December 2004 Indian Ocean tsunami. The model that we used for tsunami propagation is based on the tidal model

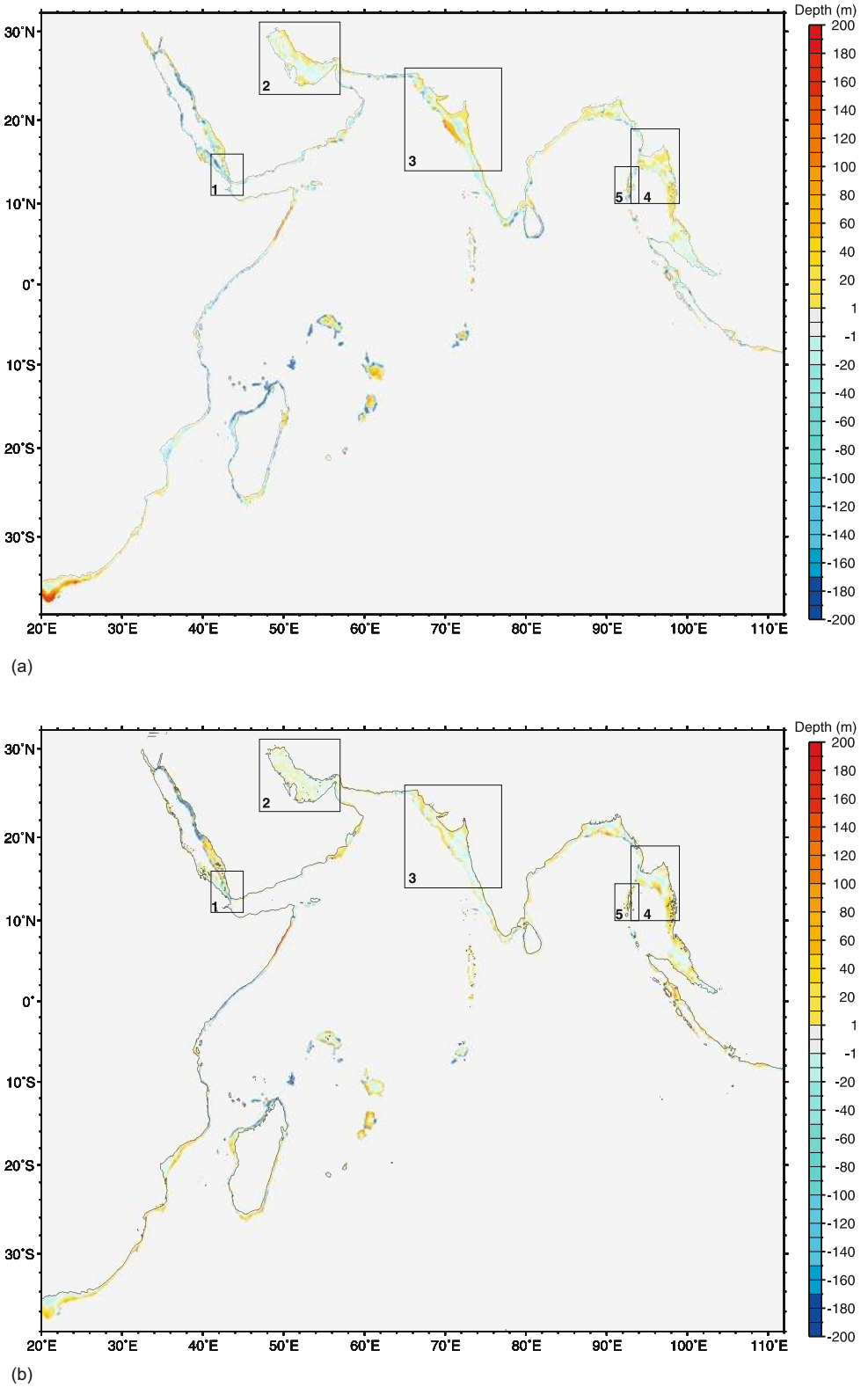

Figure 3. **(a)** The difference in depths (anomaly) between the modified ETOPO5 (ETOPO5 merged with the gridded digitized data) and the original ETOPO5 datasets for the Indian Ocean. The boxes mark the region shown in greater detail in figures 4–7. **(b)** Same as (a) but for ETOPO2 dataset.

of Unnikrishnan *et al* (1999). This model was run on 5 arc minute spatial grid resolution with the modified ETOPO5 bathymetry. The tsunami source region and the corresponding ocean surface displacement as estimated by Hirata *et al* (2006) were used as the initial condition. The new

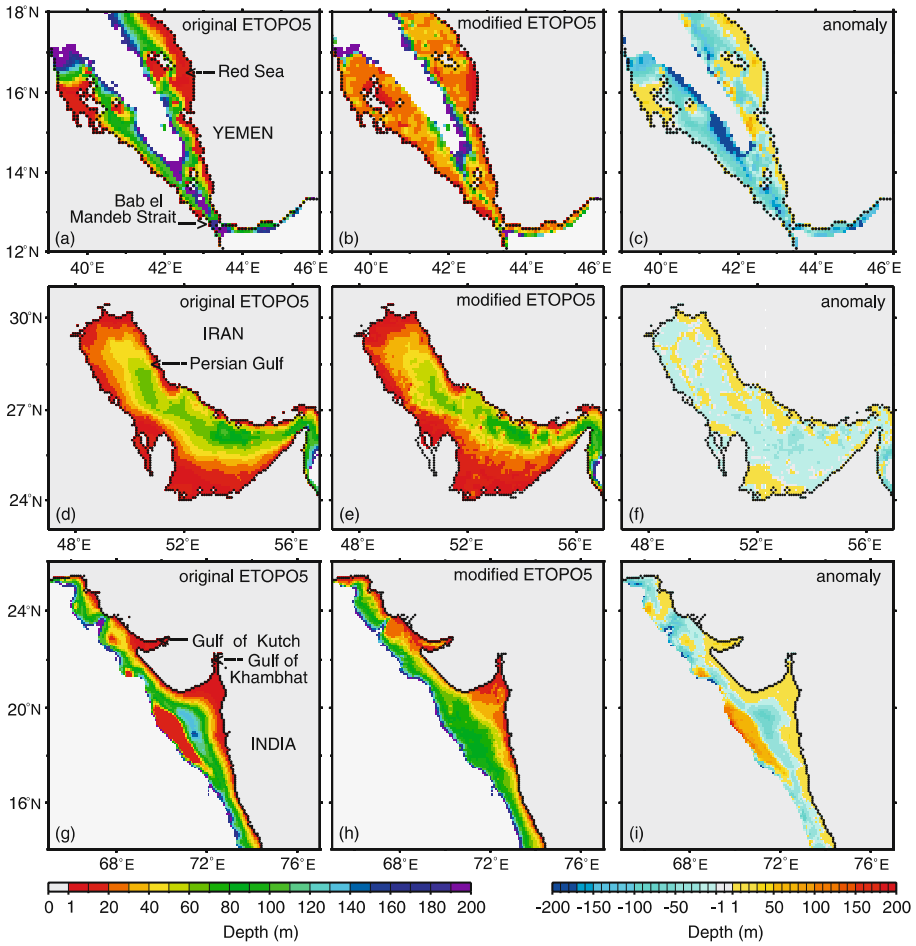

Figure 4. The bathymetry obtained from the original ETOPO5, the modified ETOPO5, and the difference between them (anomaly) for the southern Red Sea (a, b, and c respectively), for the Persian Gulf (d, e, and f respectively), and for the Gulf of Khambhat region (g, h, and i respectively).

bathymetric grid was evaluated by comparing the simulated travel times with the observed travel times (estimated from the arrival times by subtracting the time of the earthquake) at Paradip, Visakhapatnam, and Chennai which are located along the east coast of India (Nagarajan *et al* 2006).

3. Results and discussions

3.1 *Improvements in the modified bathymetry*

There was a significant improvement in the bathymetry in many regions (figures 3–7). The coastline in figures 3–7 is from the respective (original or modified) dataset. Figures 3(a) and 3(b) show the anomaly between the modified and the original bathymetric datasets for ETOPO5 and ETOPO2 respectively. The anomaly is calculated by subtracting the original depth from the modified depth. Hence, a positive (negative) anomaly implies that the depth in the original dataset was less (more) than in the modified dataset. The lower contour levels in the original ETOPO5 resulted in a positive anomaly of nearly 40–60 m in gulfs like the Gulf of Khambhat and Gulf of Martaban. High negative anomalies of about 60–80 m were found along the west coast of India and around the Madagascar Island. The ETOPO5 dataset also had a problem in representing the bathymetry near the islands and atolls and these regions showed large positive depth anomalies. Though ETOPO2v2 was similar to the modified ETOPO2 in many regions, there were still nearly 5–30 m anomalies between them in different regions. There was a negative anomaly of 5–15 m along the west coast of India and 10–40 m near the northern Bay of Bengal. High positive anomalies of nearly 100 m were found along the southern coast of Myanmar. ETOPO2v2 had high depth values near the Bab el Mandeb Strait in the Red Sea, which resulted in a high negative anomaly of nearly 200 m.

Figures 4 and 5 show the improvements in the modified ETOPO5 dataset for the Red Sea, Persian

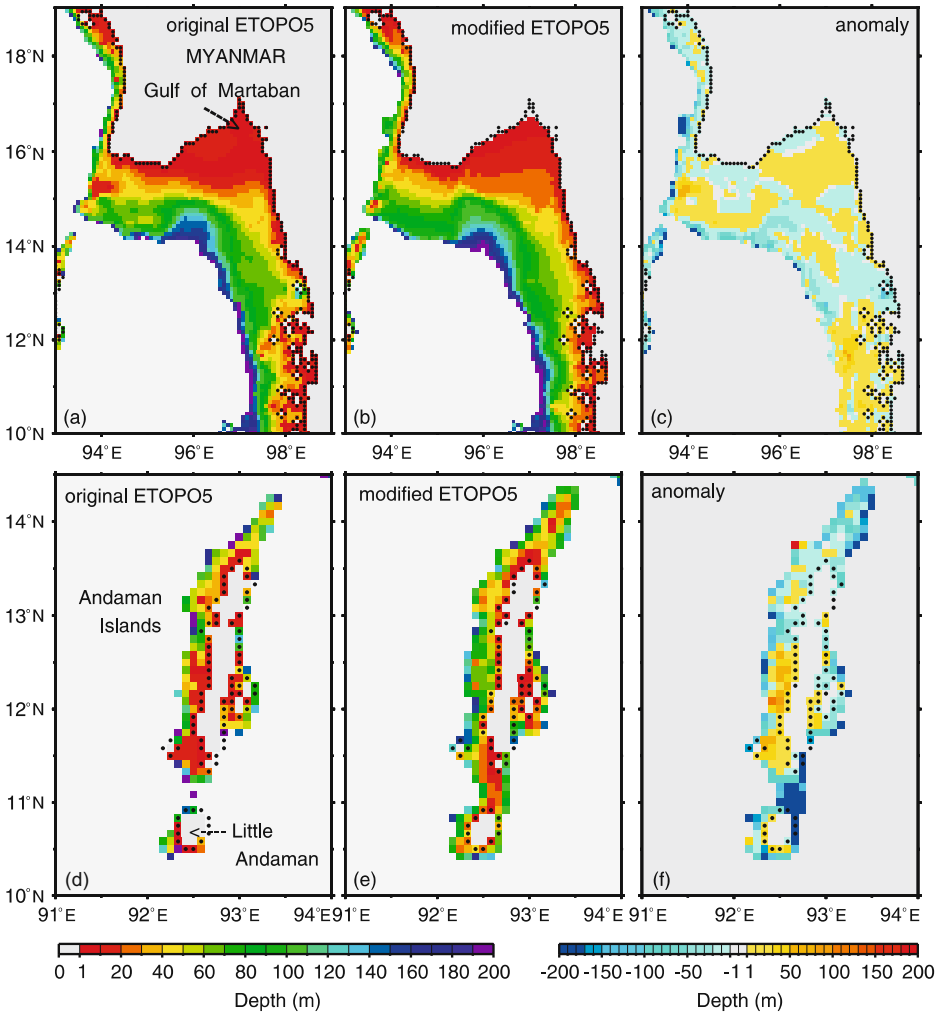

Figure 5. The bathymetry obtained from the original ETOPO5, the modified ETOPO5, and the anomaly for the Gulf of Martaban (a, b, and c respectively) and for the Andaman Islands (d, e, and f respectively).

Gulf, Gulf of Khambhat, Gulf of Martaban, and the Andaman Islands (see the boxes in figure 3). Near the Bab el Mandeb Strait in the Red Sea, the original ETOPO5 dataset had contours up to 200 m (figure 4a) throughout the narrow strait, something not found in the hydrographic charts. The bathymetry obtained from the modified dataset (figure 4b) was similar to that obtained by Maillard and Soliman (1986) during their hydrographic survey cruise in 1982. The high depth values in the ETOPO5 dataset appear as negative anomalies in figure 4(c).

In the Persian Gulf region, the original ETOPO5 (figure 4d) dataset showed depths greater than 120 m towards the coast, but the maximum depth in the gulf was around 100 m (Bower *et al* 2000). The modified dataset (figure 4e) had a maximum depth value of 90 m, a closer representation of the actual bathymetry.

In the Gulf of Khambhat region, the original ETOPO5 dataset showed a very shallow region of depth 20 m around 70.5°E, 19°N (figure 4g), thereby implying the existence of a sea-mount-like feature in the region. As evident from the hydrographic charts and the other global bathymetric grids (including ETOPO2v2), no such feature is present in that region. The modified ETOPO5 thus yielded a more realistic bathymetry for the Gulf of Khambhat (figure 4h) than the original ETOPO5 dataset. Figure 4(i) shows the improvements achieved in the modified ETOPO5.

The modified ETOPO5 dataset also represented the bathymetry of the Gulf of Martaban (figure 5a) more accurately than the original ETOPO5 dataset (figure 5b) and was similar to the bathymetry obtained by Ramaswamy *et al* (2004) from a cruise of the Ocean Research Vessel (ORV) Sagar Kanya.

The original ETOPO5 dataset showed wide shallow regions of nearly 20 m depth around the Andaman Islands (figure 5d), whereas the modified dataset showed depth variations up to $\sim$ 60 m

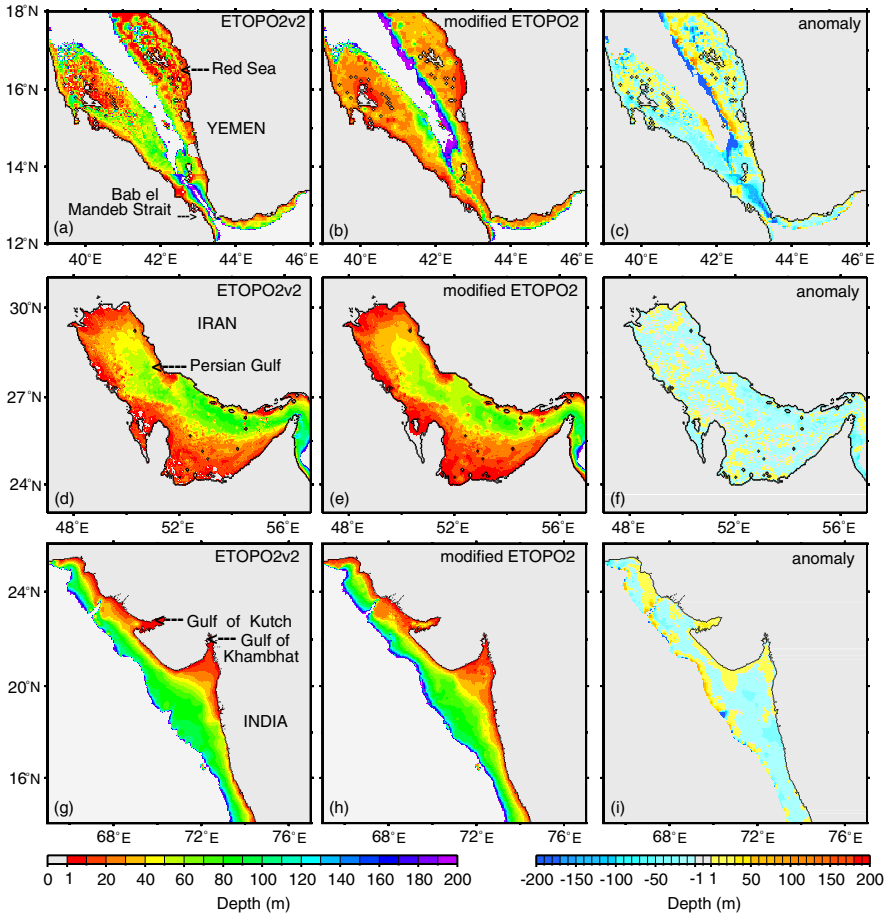

Figure 6. The bathymetry obtained from the ETOPO2v2, the modified ETOPO2, and the anomaly for the regions indicated in figure 4.

in this region (figure 5e). The depth of the sea in the region between the Andaman and the Little Andaman Islands was greater than 200 m in the original ETOPO5 (figure 5d), but in the modified bathymetry the depths here did not exceed 50 m (figure 5e). This resulted in a negative anomaly greater than 200 m (figure 5f).

Similar plots for the ETOPO2v2 and the modified ETOPO2 bathymetric grids for the above regions did not show comparable changes between the two datasets (figures 6 and 7), except for the Bab el Mandeb Strait in southern Red Sea. In this region, the ETOPO2v2 dataset showed depths greater than 200 m throughout the narrow channel (figure 6a), but the modified ETOPO2 showed depths up to 120 m (figure 6b), which is similar to that obtained by Maillard and Soliman (1986).

3.2 *Evaluation of the new bathymetry datasets*

We demonstrate the improvements in the modified datasets by carrying out numerical experiments with the models mentioned in section 2.2 using the original and the modified ETOPO datasets.

3.2.1 *Tidal model*

Figure 8 provides a comparison of the simulated sea surface elevations with the observations. At Mumbai, the comparison was poor both in amplitude and phase when the original ETOPO5 bathymetry was used, but it improved when the modified ETOPO5 was used (figure 8a). At Veraval, there was only a slight improvement in the results when the modified ETOPO5 dataset was used (figure 8b). The sea-mount-like feature in the original ETOPO5 significantly affected the simulated sea surface elevations at Mumbai. On the other hand, the simulations using the ETOPO2v2 and the modified ETOPO2 did not show any significant difference and both agreed well with the observations (figure 8c and 8d). Note that the errors in ETOPO2v2 were small near Mumbai and Veraval; there are pockets, however, where the errors were 5–25 m.

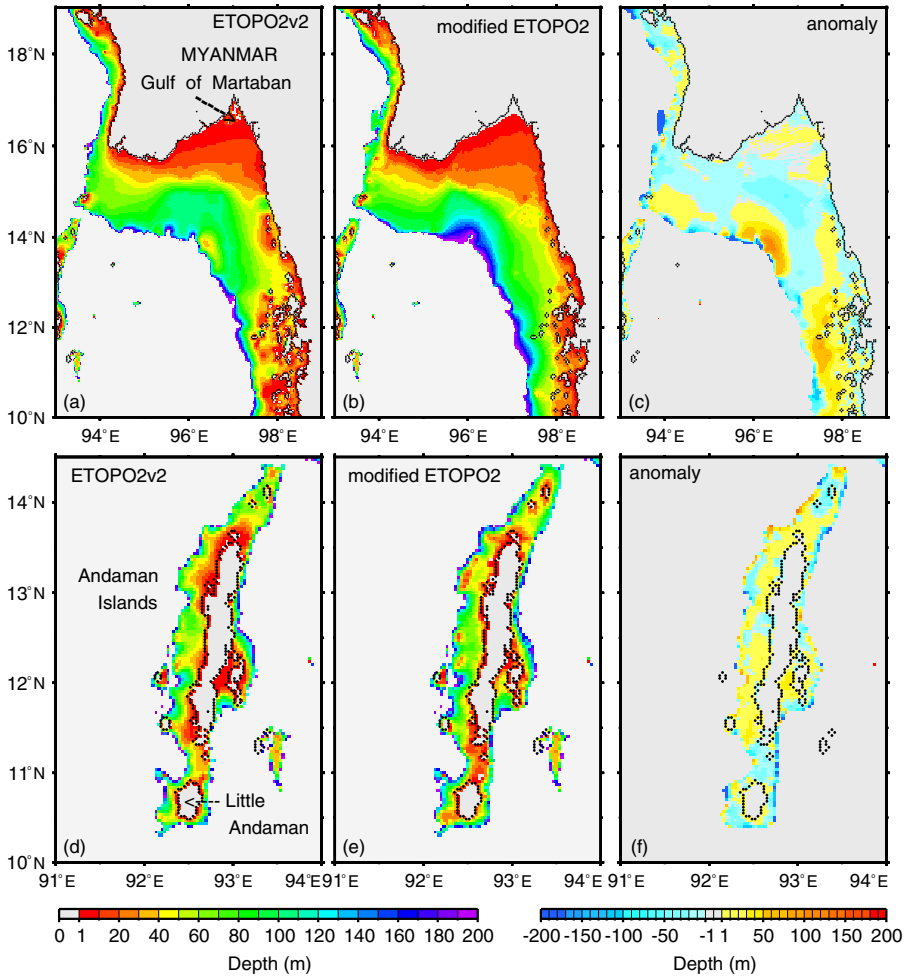

Figure 7. Same as figure 6, but for the region indicated in figure 5.

The tidal circulation in the Gulf of Khambhat and the surrounding region during high tide at Mumbai (Apollo Bandar) obtained using the original and modified ETOPO5 datasets are shown in figure 9(a) and 9(b) respectively. The significant improvement in the bathymetry of the Gulf of Khambhat and its surroundings (figure 4g and 4h) was reflected in the circulation pattern (figure 9b). The unrealistic circulation pattern in the simulation using original ETOPO5 (figure 9a) can be attributed to the presence of the unreal sea-mount-like feature present in the data. The circulation pattern obtained using the modified bathymetry (figure 9b) corresponds closely to that obtained by Unnikrishnan *et al* (1999). The circulation pattern obtained using the ETOPO2v2 and the modified ETOPO2 datasets were almost similar (figure 9c and 9d).

The comparison of the vertically averaged u and v components observed at Bombay High with that obtained from the tidal model simulation (figure 10a and 10b) clearly shows the improvement in the modified ETOPO5 bathymetric grid. The simulated u and v components obtained using the modified ETOPO5 were much closer to the observations than those obtained with the original ETOPO5. However, the predicted components obtained using the modified ETOPO2 were similar to those obtained using the ETOPO2v2 (figure 10c and 10d).

3.2.2 *Tsunami model*

Tide-gauge records at Paradip, Visakhapatnam, and Chennai during the occurrence of 2004 Indian Ocean tsunami show that the tsunami waves arrived at the east coast of India in about 150 minutes after the earthquake (Nagarajan *et al* 2006). Figure 11 shows a snapshot of the simulation at 150 minutes after the origin time of earthquake. The model grid point closest to the tide-gauge location was used for comparing the tsunami travel times. The simulated tsunami travel times are within ±10 minutes error with the observed travel times. This is a good agreement keeping in mind the coarse grid (5 arc minutes) used for the tsunami

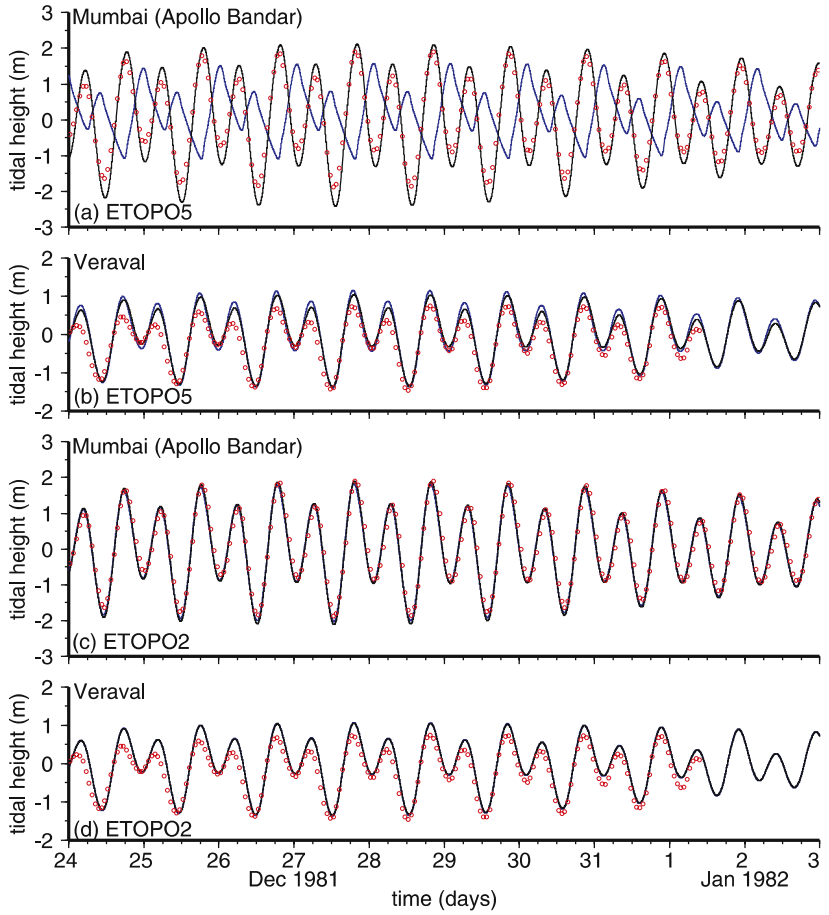

Figure 8. The sea surface elevation observed (red dots) at Mumbai (Apollo Bandar) **(a)** and Veraval **(b)** obtained from a simulation of the tidal model when the original ETOPO5 dataset (blue line) and the modified dataset (black line) are used. Panels (c) and (d) are the same as (a) and (b) but for ETOPO2 dataset.

modelling. Similar agreement (±10 minutes) was also obtained in the simulation using the original ETOPO5 dataset because the differences between the two bathymetry datasets in the shelf along the east coast of India are of the order of 5–20 m which does not affect the tsunami arrival times significantly on a 5 arc minute grid. The differences were of the same order along the east coast of India when comparing the modified ETOPO2 with the ETOPO2v2.

Tsunami modelling on a coarse grid of 5 arc minutes is useful for determining the approximate tsunami arrival times at the coast and to study the general characteristics of tsunami propagation. It is not, however, sufficient to resolve the high-frequency components of the tsunami waves. In order to determine the tsunami waveforms accurately, one needs to have a grid as fine as 20 arc seconds near the coast, which requires interpolation from a coarser grid because no bathymetry dataset is available at the required resolution. Though we do not see significant differences in the model runs using the original and modified ETOPO5 datasets, the depth differences of 5–20 m near the coast would be significant if the ETOPO5 dataset was used as the source for interpolating to a fine grid. These errors would significantly affect the tsunami waveforms. Hence, the modified datasets (including the modified ETOPO2) will be useful in deriving the bathymetry on a fine grid, as the shelf bathymetry is better represented by them.

From the discussions above, it is evident that the modified ETOPO datasets are an improvement over the original ETOPO datasets. A drawback of the modified datasets, however, is that the maps used for digitization are of different resolutions which leads to sparse data in some regions.

4. Conclusion

Improved 5 arc minute and 2 arc minute bathymetric datasets derived from digitized contours and sounding depths values have been developed for the entire Indian Ocean north of 38°S and

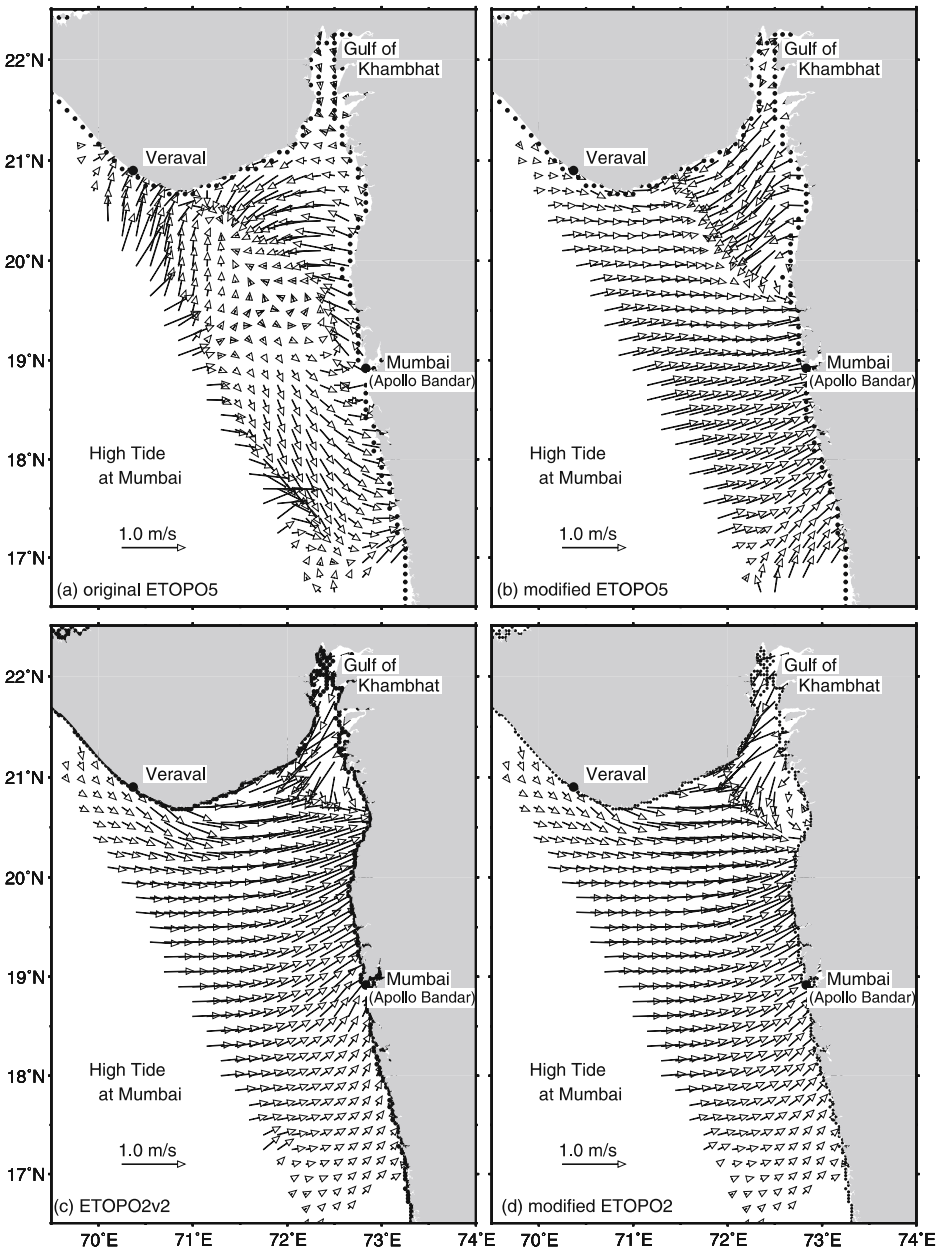

Figure 9. The simulated tidal circulation in the Gulf of Khambhat and the surrounding region corresponding to the time of occurrence of high tide at Mumbai (Apollo Bandar) obtained by using the **(a)** original ETOPO5, **(b)** modified ETOPO5 dataset, **(c)** ETOPO2v2, and **(d)** modified ETOPO2 dataset.

between 20°E and 112°E. The original ETOPO5 bathymetry data was shown to be inaccurate for shallow regions. The new version of the ETOPO2 (ETOPO2v2) dataset was validated. Though the errors in ETOPO2v2 dataset are comparatively much smaller, there are still high anomalies between the ETOPO2v2 and modified ETOPO2 datasets especially in the Red Sea region and along the southern coast of Myanmar. In order to generate the modified datasets, the shallow depth values (less than 200 m) derived from the hydrographic charts were gridded and then blended with the deeper depth values (greater than 200 m) from the original ETOPO datasets using an appropriate merging technique to ensure smooth transition across the boundary between the two datasets. The improvements of the modified datasets over the original ETOPO datasets have been demonstrated using a tidal circulation model and a tsunami propagation model, thereby, assuring the modellers that they have a more accurate (in depths less than 200 m) common dataset for the Indian Ocean region. The modified ETOPO5 and the modified ETOPO2 bathymetric datasets are available at http://www.nio.org/data_info/bathymetry/modified-etopo.htm.

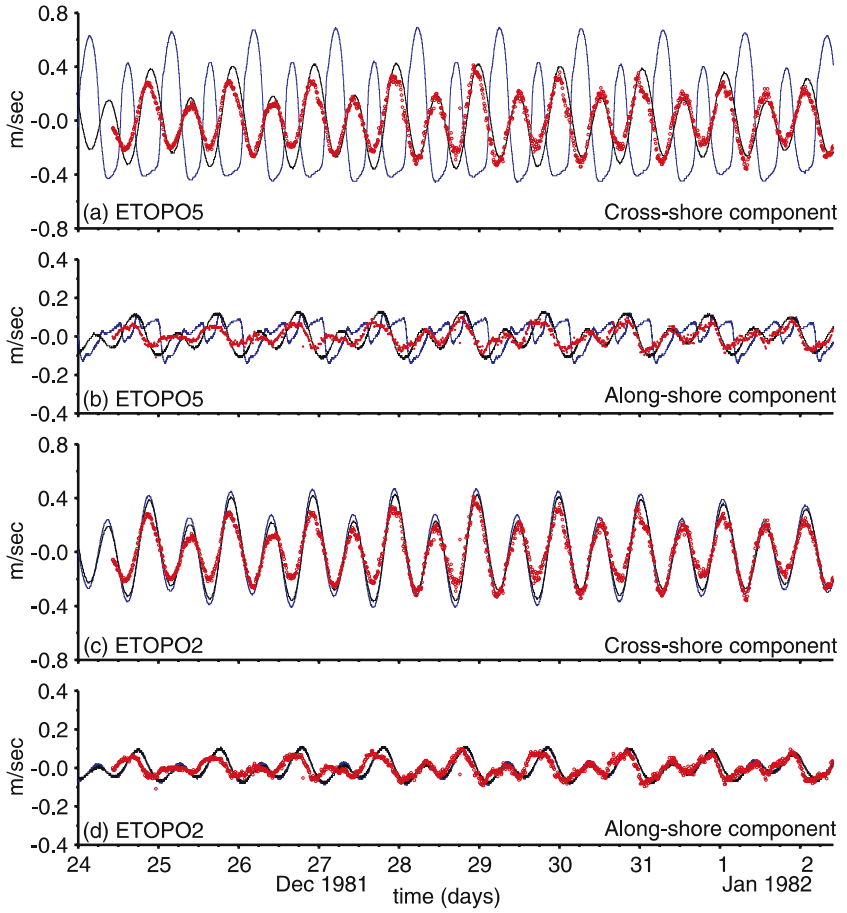

Figure 10. The vertically averaged cross-shore **(a)** and along-shore **(b)** components computed from the observed current (red dots) at Bombay High and that simulated by the tidal model during 24 December 1981 to 3 January 1982 when the original (blue line) and the modified ETOPO5 (black line) is used. Panel **(c)** and **(d)** are the same as **(a)** and **(b)** but for ETOPO2 dataset.

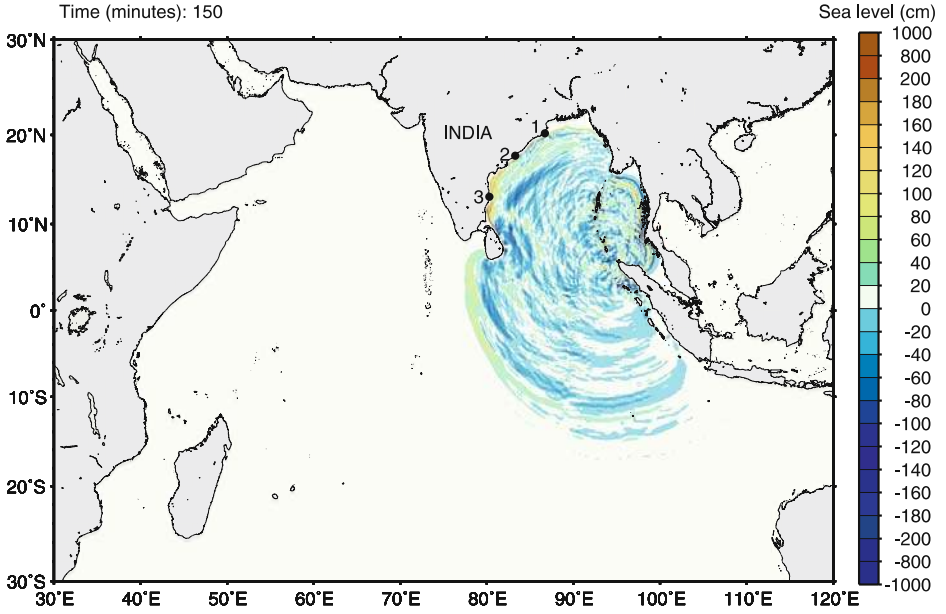

Figure 11. A snapshot of the tsunami simulation using the modified ETOPO5 dataset 150 minutes after the earthquake. Paradip, Visakhapatnam, and Chennai are marked as 1, 2, and 3 respectively.

Acknowledgements

The first author thanks CSIR for providing a fellowship. The authors also thank D Shankar and S S C Shenoi for their useful suggestions. We thank the referees Yushiro Fujii and Karen Marks for their critical reviews which helped to improve the manuscript. The present work was supported by funds from INCOIS (Indian National Centre for Ocean Information Services), Government of India. This is NIO Contribution 4248.

References

Ahuja A K 2000 Country report on the current status of surveying, mapping and cartographic activities, Fifteenth United Nations regional cartographic conference for Asia and the Pacific, Kuala Lumpur.

Bower A S, Hunt H D and Price J 2000 Character and Dynamics of the Red Sea and Persian Gulf Outflows; *J. Geophys. Res.* **105** 6387–6414.

Divins D L and Metzger D 2003 NGDC Coastal Relief Model, National Geophysical Data Center (http://www.ngdc.noaa.gov/mgg/coastal/coastal.html).

Fujii Y and Satake K 2007 Tsunami source of the 2004 Sumatra–Andaman earthquake inferred from tide gauge and satellite data; *Bull. Seismol. Soc. Am.* **97** S192–S207.

Goodwillie A and working group of GEBCO Sub-Committee on Digital Bathymetry 2003 Centenary Edition of the GEBCO digital Atlas; *User Guide to the GEBCO one minute grid* (http://www.bodc.ac.uk/data/online_delivery/gebco).

GRASS Development Team 2005 GRASS 6.0 Users Manual ITC-irst, Trento, Italy (http://grass.itc.it/grass60/manuals/html60_user).

Hastings D A, Dunbar P K, Elphingstone G M, Bootz M, Murakami H, Holland P, Bryant N A, Logan T L, Muller J P, Schreier G and MacDonald J S (eds) 1998 The Global Land One-kilometer Base Elevation (GLOBE) Digital Elevation Model, Version 1.0; *National Oceanic and Atmospheric Administration, National Geophysical Data Center*, Boulder, Colorado, USA (http://www.ngdc.noaa.gov/mgg/topo/globe.html).

Hirata K, Satake K, Tanioka Y, Kuragano T, Hasegawa Y, Hayashi Y and Hamada N 2006 The 2004 Indian Ocean tsunami: Tsunami source model from satellite altimetry; *Earth Planets Space* **58(2)** 195–201.

IHO 1987 *IHO Standards for Hydrographic Surveys*, Special publication 44, International Hydrographic Organisation, 3rd edition, International Hydrographic Bureau, Monaco.

Jakobsson M, Cherkis N Z, Woodward J, Macnab R and Coakley B 2000 New grid of Arctic bathymetry aids scientists and mapmakers; *EOS, Trans. Am. Geophys. Union* **81** 89–96.

Lay T, Kanamori H, Ammon C J, Nettles M, Ward S N, Aster R C, Beck S L, Bilek S L, Brudzinski M R, Butler R, DeShon H R, Ekström G, Satake K and Sipkin S 2005a The Great Sumatra–Andaman Earthquake of 26 December 2004; *Science* **308** 1127.

Lay T, Kanamori H, Ammon C J, Nettles M, Ward S N, Aster R C, Beck S L, Bilek S L, Brudzinski M R, Butler R, DeShon H R, Ekström G, Satake K and Sipkin S 2005b Response to Comments on "The Great Sumatra–Andaman Earthquake of 26 December 2004"; *Science* **310** 1431b.

Maillard C and Soliman G 1986 Hydrography of the Red Sea and exchanges with the Indian Ocean in summer; *Ocean. Acta* **9** 249–269.

Mills G B 1998 International Hydrographic Surveys Standards; *International Hydographic Review* **75** 79–86.

Nagarajan B, Suresh I, Sundar D, Sharma R, Lal A K, Neetu S, Shenoi S S C, Shetye S R and Shankar D 2006 The Great Tsunami of 26 December 2004: A description based on tide-gauge data from the Indian subcontinent and the surrounding areas; *Earth Planets Space* **58(2)** 211–215.

National Geophysical Data Center 1988 *Data announcement 88-MGG-02*, Digital relief of the Surface of the Earth, Natl. Oceanic and Atmos. Admin., US Dept. Commerce, Boulder, Colorado, USA.

National Geophysical Data Center 2006 2-minute Gridded Global Relief Data (ETOPO2v2), Natl. Oceanic and Atmos. Admin., U. S. Dept. of Commerce (http://www.ngdc.noaa.gov/mgg/fliers/06mgg01.html).

National Oceanic and Atmospheric Administration 2001 Great Lakes Bathymetry, U.S. Dept. of Commerce (http://www.ngdc.noaa.gov/mgg/greatlakes/greatlakes.html).

Neetu S, Suresh I, Shankar R, Shankar D, Shenoi S S C, Shetye S R, Sundar D and Nagarajan B 2005 Comments on "The Great Sumatra–Andaman Earthquake of 26 December 2004"; *Science* **310** 1431a.

Neteler M and Mitasova H 2002 *Open Source GIS: A GRASS GIS Approach*, Kluwer Academic Publishers, Kluwer, New York; 225.

Ramaswamy V, Rao P S, Rao K H, Thwin S, Rao N S and Raiker V 2004 Tidal influence on suspended sediment distribution and dispersal in the northern Andaman Sea and Gulf of Martaban; *Mar. Geol.* **208** 33–42.

Satake K 1988 Effects of bathymetry on tsunami propagation: Application of Ray tracing to tsunamis; *PAGEOPH* **126(1)** 27–36.

Smith W H F and Sandwell D T 1997 Global sea floor topography from satellite altimetry and ship depth soundings; *Science* **277** 5334.

Smith W H F and Wessel P 1990 Gridding with continuous curvature splines in tension; *Geophysics* **55** 293–305.

Unnikrishnan A S, Shetye S R and Michael G S 1999 Tidal propagation in the Gulf of Khambhat, Bombay High, and surrounding areas; *Proc. Indian Acad. Sci.* (*Earth Planet. Sci.*) **108** 155–177.

US National Geospatial-Intelligence Agency 1994 Digital Bathymetric Data Base (DBDB) 5 minute, Fairfax (Virginia), DMA.

Van der Wal D and Pye K 2003 The use of historical bathymetric charts in a GIS to assess morphological change in estuaries; *The Hydrographic Journal* **110** 3–9.

Vatsa G S and Rajesh Kumar 2002 Coastal Mapping and Marine Charts; *Indian Cartographer* **22** 157–161.

Vatsa G S, Singh U K, Doss C M and Gupta M P 2002 Convergence of Hydrographic Information in Nautical charts; *Indian Cartographer* **22** 166–171.

Wessel P and Smith W H F 1995 New version of the Generic Mapping Tools released; *EOS Trans. Amer. Geophys. Un.* **76** 329 (http://www.agu.org/eos_elec/95154e.html).

Wessel P and Smith W H F 1998 New improved version of GMT released; *EOS Trans. Amer. Geophys. Un.* **79** 579.

MS received 13 July 2006; revised 2 March 2007; accepted 12 April 2007